

Cite this article as: Shao Wenting, Wu Xiangyu, Jiang Bailing, et al. Conductive and Corrosion-Resistant Properties of Graphite-like Carbon Coating on 6061 Aluminum Alloy Bipolar Plate for Proton Exchange Membrane Fuel Cell[J]. Rare Metal Materials and Engineering, 2022, 51(01): 1-5.

LETTER

Conductive and Corrosion-Resistant Properties of Graphite-like Carbon Coating on 6061 Aluminum Alloy Bipolar Plate for Proton Exchange Membrane Fuel Cell

Shao Wenting¹, Wu Xiangyu¹, Jiang Bailing², Chen Jian¹, Yang Wei¹

¹Xi'an Technological University, Xi'an 710021, China; ²Xi'an University of Technology, Xi'an 710048, China

Abstract: In order to obtain the critical thickness of graphite-like carbon coating on 6061 aluminum alloy with the corrosion resistance against proton acid and the reduction value of interfacial contact resistance, a series of graphite-like carbon coatings were deposited on 6061 aluminum alloy plate by a magnetron sputtering system. The microstructure of the deposited coatings was characterized, and the interfacial contact resistance, corrosion resistance, and stability of the coatings were analyzed. Results show that the critical thickness of the graphite-like carbon coating on 6061 aluminum alloy with corrosion resistance against the proton acid in proton exchange membrane fuel cell cathode environment is 0.97 μm . Compared with the ones prepared at low carbon target currents, the coatings prepared at the carbon target current of 4.5 A show a smoother surface. When the carbon target current reaches 4.5 A, the interfacial contact resistance is the lowest, reaching 16 $\text{m}\Omega\cdot\text{cm}^2$, which is two times larger than that of the graphite bipolar plate.

Key words: graphite-like carbon coating; aluminum alloy bipolar plate; interfacial contact resistance; corrosion resistance

Proton exchange membrane fuel cell (PEMFC) is attractive due to its advantages of high conversion efficiency, reduced emission, and quick start^[1-3]. Bipolar plate is the key part of PEMFCs, which occupies nearly 80% of the total mass or volume^[3,4]. However, the thickness of traditional graphite bipolar plates is 2 mm, which is hard to meet the requirements of lightweight or small volume for vehicle battery. Using aluminum alloy plate with the thickness of less than 0.5 mm instead of the graphite plate with thickness of 2 mm can reduce the mass and volume of PEMFC by more than 50%, and the decrement has become the main competitive index of PEMFC for vehicles. Nevertheless, the poor corrosion resistance of the aluminum alloy plate^[3,5] not only leads to the increase of interfacial contact resistance (ICR), but also results in the contamination of membrane electrodes, which undoubtedly reduces the performance of the fuel cell. Therefore, a protective coating on aluminum alloy plates to meet both conductive and corrosion-resistant requirements^[6] is fundamental in the metallization of the fuel cell bipolar plates.

Graphite-like carbon (GLC) coating is a type of amorphous carbon with a large number of sp^2 bonds, which has been widely used in surface modification because of its excellent conductivity and high chemical stability^[7-11]. Yi et al^[8] prepared a series of amorphous carbon (a-C) coatings on the surface of stainless steel, and the results showed that ICR and corrosion current density are much lower than the target values of the Department of Energy (DOE)^[6]. Larijani et al^[12] compared the carbon-coated and uncoated 316L stainless steel in PEMFCs, and the results showed that the carbon-coated 316L stainless steel has a lower corrosion rate. Bi et al^[13] also prepared the a-C coating on 316L stainless steel, and the results showed that ICR is much lower than that of the DOE target^[6]. However, the conductive and corrosion-resistant properties of GLC coatings on 6061 aluminum alloy bipolar plates are rarely investigated. Therefore, it is of great significance to study the critical thickness of GLC coatings on 6061 aluminum alloy bipolar plates with corrosion resistance against proton acid in PEMFC cathode environment and to

Received date: January 10, 2021

Foundation item: China Postdoctoral Science Foundation (2020M683670XB); National Innovation Project of Xi'an Technological University (S202010702037)

Corresponding author: Shao Wenting, Ph. D., Lecturer, School of Materials Science and Chemical Engineering, Xi'an Technological University, Xi'an 710021, P. R. China, Tel: 0086-29-86173324, E-mail: wenting@xatu.edu.cn

Copyright © 2022, Northwest Institute for Nonferrous Metal Research. Published by Science Press. All rights reserved.

obtain the decrement of ICR.

In this research, a series of GLC coatings were prepared on 6061 aluminum alloy substrates by a magnetron sputtering system. The microstructure and the conductive and corrosion-resistant properties of the GLC coatings were studied. The critical thickness of GLC coatings on 6061 aluminum alloy bipolar plates for corrosion resistance against proton acid was obtained and the ICR decrement was determined. The results provided an experimental and theoretical support for the mass reduction of PEMFC.

1 Experiment

GLC coatings were deposited using a MSIP-019 magnetron sputtering system. The 6061 aluminum alloy specimen with diameter of 40 mm and the single crystal silicon were used as substrates. The targets containing high purity (99.99%) carbon and chromium with the diameter of 100 mm were installed in the cylindrical furnace chamber, and the sputtering area was approximately 50 cm². The specimens were placed vertically into the specimen holders with the rotation speed of 8 r/min and the distance between the target and specimen was 90 mm.

Before the experiment, the pressure of the vacuum chamber was pumped down to 3.0×10^{-3} Pa. Then a plasma cleaning process was performed with a carbon target current of 0.1 A, a Cr target current of 0.3 A, and a bias voltage of -400 V for 20 min. Subsequently, a pure Cr interlayer of about 100 nm in thickness was prepared to improve the bonding strength between the coating and substrate. GLC coatings were prepared by changing the carbon target current from 1.0 A to 4.5 A, and the bias voltage was fixed at -60 V. The deposition time was 180 min. The flow of working gas Ar (purity of 99.999%) was controlled at 40 mL/min to maintain the working pressure of 10^{-1} Pa.

The coating thickness was measured by scanning electron microscope (SEM) and the deposition rate was determined according to the coating thickness and deposition time. The 2D and 3D morphologies of GLC coatings were characterized by atomic force microscopy (AFM). The Ar⁺ laser of 532 nm in wavelength with a resolution of 1 cm⁻¹ was used to obtain the Raman spectra in the range of 800~1800 cm⁻¹ by Raman spectrometer. The laser power density on the specimen was less than 1 mW·mm⁻² to avoid possible beam-induced graphitization. The bonding states of carbon atoms in GLC coatings were analyzed by X-ray photoelectron spectroscopy (XPS). Before XPS analysis, the argon ion beam of 4 keV was used to etch the specimen surface for 5 min in order to avoid the influence of surface contamination. The corrosion resistance of GLC coatings on 6061 aluminum alloy substrates was characterized by CHI-670 electrochemical workstation in the cathode environment of PEMFCs (80 °C, 0.5 mol·L⁻¹ H₂SO₄+5 mg·L⁻¹ F⁻). The ICR between the coating and carbon paper (Toray-060) was measured using a ZY-9858 digital ohmmeter and a YC-611 universal tester coupled with gold-plated copper electrodes.

2 Results and Discussion

2.1 Thickness and deposition rate of GLC coatings

Fig.1 illustrates the relationship between the thickness and deposition rate of GLC coatings with the carbon target currents. As shown in Fig.1, with increasing the carbon target current from 1.0 A to 4.5 A, the thickness of coatings is gradually increased from 0.44 μm to 1.49 μm, and the deposition rate of the coating is increased from 2.44 nm·min⁻¹ to 8.32 nm·min⁻¹. The increment of thickness and deposition rate is large firstly and then becomes small, indicating that the increasing trend slows down. It is well known that the deposition rate of the coating is closely related to the sputtering rate of target materials. The higher the carbon target current, the more the ions sputtered from the carbon target surface, and the thicker the GLC coating. However, with increasing the carbon target current, it is more likely to produce a back-sputtering phenomenon under the bombardment of deposited particles, which leads to the slower increasing trend in deposition rate. Therefore, the critical thickness of GLC coating is 0.97 μm when the carbon target current is 1.5 A.

2.2 Microstructure of GLC coatings

Fig.2 shows the 2D and 3D AFM images of GLC coatings obtained under different carbon target currents. It can be seen that the diameter of carbon clusters is firstly increased and then decreased with increasing the carbon target current from 1.0 A to 4.5 A. This is because the sputtering atoms are attached to the previously formed island-like cluster particles at the beginning and the carbon clusters gradually grow. When the carbon target current increases to 4.5 A, the coatings exhibit a smooth surface with carbon clusters of 50 nm in diameter distributed on the surface. The differences in 2D and 3D morphologies are associated with the ion energy input during deposition. The high input of ion energy is conducive to the movement or diffusion of the deposited atoms, thus leading to a smoother surface. The ion energy is associated with the ion bombardment effect and can produce heating effect^[14].

Fig. 3 shows Raman spectra of GLC coatings obtained

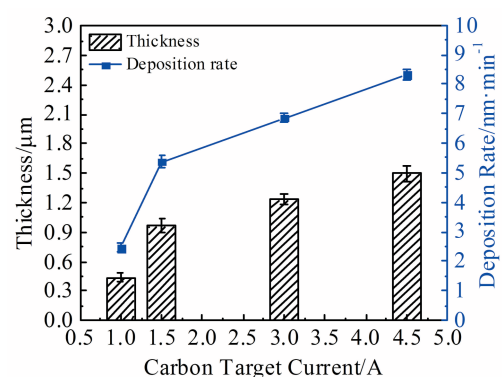


Fig.1 Relationship of thickness and deposition rate of GLC coatings with carbon target current

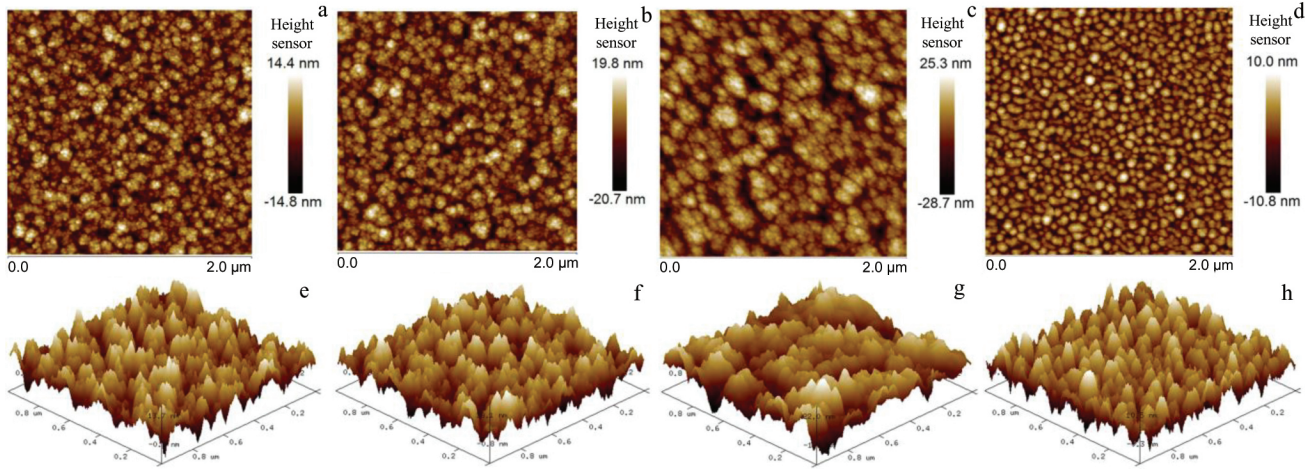


Fig.2 2D (a~d) and 3D (e~h) AFM images of GLC coatings at different carbon target currents: (a, e) 1.0 A, (b, f) 1.5 A, (c, g) 3.0 A, and (d, h) 4.5 A

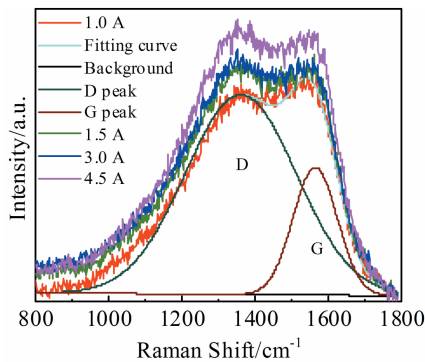


Fig.3 Raman spectra of GLC coatings at different carbon target currents

under different carbon target currents. It can be seen that the Raman spectra of the coatings have an intensive D band at around 1360 cm^{-1} and a weak G band at around 1560 cm^{-1} . The detailed fitting results of Raman spectra are presented in Table 1. The I_D/I_G presents the size of sp^2 phase of ring structure, while the position and full width at half maximum (FWHM) of G peak indicate the disorder of the coating^[15-17]. As shown in Table 1, the value of I_D/I_G is firstly increased from 3.92 to 4.18 and then decreased to 3.82 with increasing the carbon target current from 1.0 A to 4.5 A, which indicates that the number of sp^2 phase clusters of ring structure is firstly increased and then decreased^[17,18]. Meanwhile, the G peak position increases from 1562.77 cm^{-1} to 1570.43 cm^{-1} and the FWHM of G peak decreases from 142.13 cm^{-1} to 136.06 cm^{-1} . This result suggests that the disordered degree of the coatings is reduced.

Fig. 4 shows the C 1s spectra of GLC coatings obtained under different carbon target currents. The C 1s spectra contain a large asymmetric peak which suggests the presence of carbon atoms in different bonding states^[19]. As shown in Fig.4, the C 1s peak broadband contains the sp^2 bond peak, sp^3 bond peak, and C-O peak at 284.4, 285.2, and 286.8 eV,

Table 1 Fitting results of Raman spectra in Fig.3

Carbon target current/A	G peak		I_D/I_G
	Peak position/ cm^{-1}	FWHM/ cm^{-1}	
1.0	1562.77	142.13	3.92
1.5	1567.12	140.74	4.02
3.0	1567.35	138.10	4.18
4.5	1570.43	136.06	3.82

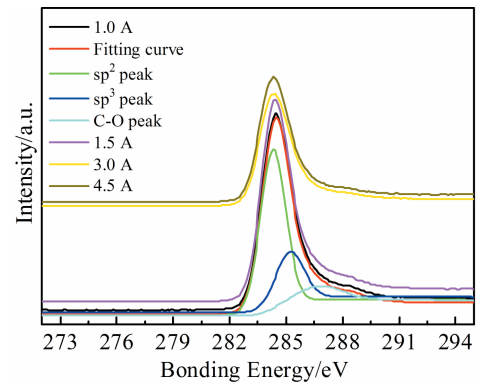


Fig.4 C 1s spectra of GLC coatings at different carbon target currents

respectively. The sp^2 bond is the main composition of the coatings, which is the typical characteristic of GLC coatings. After peak fitting, the fraction of sp^2 bond, sp^3 bond, and C-O bond of the deposited coatings was calculated, as shown in Table 2. It can be seen that the proportion of sp^2 bond is firstly increased from 62.17% to 74.71% and then decreased to 49.96%, while the proportion of sp^3 bond is firstly decreased from 22.69% to 11.55% and then increased to 42.74%, with increasing the carbon target current from 1.0 A to 4.5 A. The increase of sp^2 bond fraction is attributed to the increase of carbon target current. With increasing the carbon target current, the high-energy ions promote the graphitization and the sp^2 clusters grow. These results are in accordance with the Raman spectra analysis. However, when the carbon target

Table 2 Fitting results of C1s spectra in Fig.4

Carbon target current/A	Fraction of sp ² /%	Fraction of sp ³ /%	Fraction of C-O/%
1.0	62.17	22.69	15.19
1.5	65.39	16.28	18.33
3.0	74.71	11.55	13.73
4.5	49.96	42.74	7.29

current is increased to 4.5 A, the incident ion has enough energy to penetrate the subsurface, which is conducive to the formation of sp³ clusters.

2.3 Corrosion resistance of uncoated and GLC-coated 6061 aluminum alloys

Fig. 5 presents the potentiodynamic polarization curves of uncoated and GLC-coated 6061 aluminum alloy in the simulated cathode environment of PEMFCs, and the corresponding corrosion potential and corrosion current density are presented in Table 3. The corrosion current density of the GLC-coated 6061 aluminum alloy is 2~3 orders of magnitude lower than that of the uncoated 6061 aluminum alloy ($4.43 \times 10^{-4} \text{ A} \cdot \text{cm}^{-2}$). As the carbon target current increases from 1.0 A to 4.5 A, the corrosion current density of the GLC-coated 6061 aluminum alloy is decreased from $2.39 \times 10^{-6} \text{ A} \cdot \text{cm}^{-2}$ to $2.74 \times 10^{-7} \text{ A} \cdot \text{cm}^{-2}$, and the corrosion potential becomes more and more positive from -0.54 V to -0.12 V . The results indicate that the corrosion resistance is improved in the order of uncoated aluminum alloy < GLC-coated specimen at 1.0 A < GLC-coated specimen at 1.5 A < GLC-

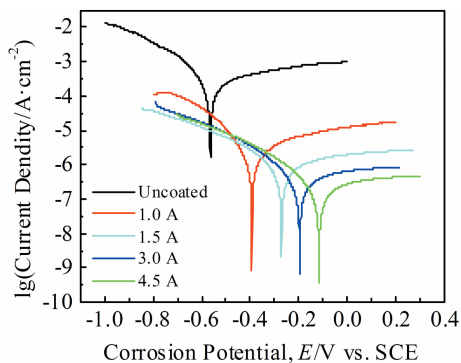


Fig.5 Potentiodynamic polarization curves of uncoated and GLC-coated 6061 aluminum alloys

Table 3 Corrosion potential and corrosion current density of uncoated and GLC-coated 6061 aluminum alloys

Specimen	Carbon target current/A	Corrosion potential/V	Corrosion current density/A·cm ⁻²
Uncoated	-	-0.54	4.43×10^{-4}
	1.0	-0.39	2.39×10^{-6}
GLC-coated	1.5	-0.28	7.79×10^{-7}
	3.0	-0.20	4.28×10^{-7}
	4.5	-0.12	2.74×10^{-7}

coated specimen at 3.0 A < GLC-coated specimen at 4.5 A. The results are mainly attributed to the coating thickness: the GLC coating with a thickness of only 0.97 μm can meet the corrosion resistance requirement of DOE targets.

Fig. 6 shows the relationship between corrosion current density and time of uncoated and GLC-coated 6061 aluminum alloys polarized at +0.6 V vs. Ag/AgCl reference electrode in the simulated cathode environment of PEMFC. The plot of uncoated aluminum alloy presents that the corrosion current density is high at the beginning and becomes stable after $8 \times 10^3 \text{ s}$. The decrease of corrosion current density is due to the formation of passivation film on aluminum alloy surface. Moreover, the potentiostatic plots of GLC-coated 6061 aluminum alloys show that the corrosion current density is gradually increased and become stable after $2 \times 10^3 \text{ s}$. The GLC coating obtained at the carbon target current of 4.5 A has the lowest corrosion current density.

2.4 ICR of uncoated and GLC-coated 6061 aluminum alloys

Fig. 7 presents the relationship between ICR of uncoated and GLC-coated 6061 aluminum alloys and compaction force. It can be seen that the curves of ICR show a decreasing trend with increasing the compaction force, because the real contact area between the coating and carbon paper expands. As the

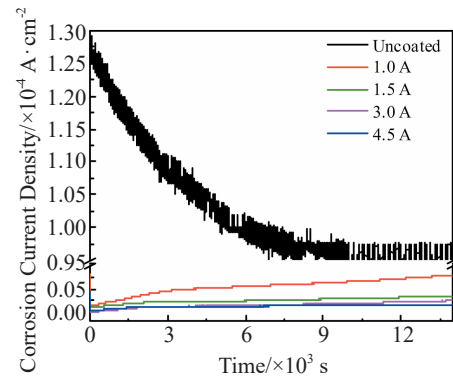


Fig.6 Potentiostatic polarization curves of uncoated and GLC-coated 6061 aluminum alloys

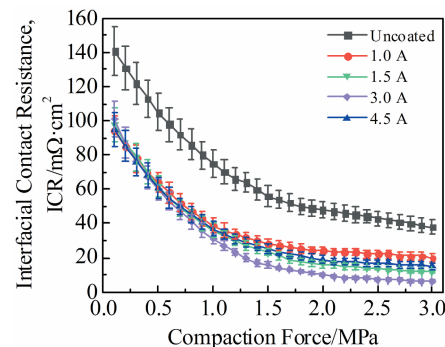


Fig.7 ICR of uncoated and GLC-coated 6061 aluminum alloys at different compaction forces

compaction force increases to a certain extent, the deformation of the coating becomes infinitesimal, the real contact area remains unchanged, and ICR becomes stable. Under the compaction force of 1.5 MPa, ICR of uncoated aluminum alloy is $56 \text{ m}\Omega \cdot \text{cm}^2$ and the ICR of GLC-coated 6061 aluminum alloy is firstly reduced from $28 \text{ m}\Omega \cdot \text{cm}^2$ to $16 \text{ m}\Omega \cdot \text{cm}^2$ and then increased to $25 \text{ m}\Omega \cdot \text{cm}^2$ with increasing the carbon target current from 1.0 A to 4.5 A. The lowest ICR of GLC coating on 6061 aluminum alloy is two times larger than that of graphite bipolar plate. The above results indicate that the ICR is closely associated with the fraction of sp^2 bonds in the coating.

3 Conclusions

1) The critical thickness of graphite-like carbon (GLC) coating on 6061 aluminum alloy substrate with corrosion resistance against the cathode environment of proton exchange membrane fuel cell (PEMFC) is $0.97 \mu\text{m}$.

2) The proportion of sp^2 bonds is firstly increased and then decreased with increasing the carbon target current.

3) The lowest interfacial contact resistance of GLC coating on 6061 aluminum alloy is two times larger than that of graphite bipolar plate.

References

- 1 Wang Y, Diaz D F R, Chen K S et al. *Materials Today*[J], 2020, 32: 178
- 2 Liu Y X, Hua L. *Journal of Power Sources*[J], 2010, 195(11): 3529
- 3 Gutiérrez A G G, Sebastian P J, Cacho L M et al. *International Journal of Electrochemical Science*[J], 2018, 13: 3958
- 4 Silva R F, Franchi D, Leone A et al. *Electrochimica Acta*[J], 2006, 51(17): 3592
- 5 Wu Xiaoquan, Yan Hong, Xin Yong et al. *Rare Metal Materials and Engineering*[J], 2020, 49(8): 2574
- 6 Asri N F, Husaini T, Sulong A B et al. *International Journal of Hydrogen Energy*[J], 2017, 42(14): 9135
- 7 Hou K, Yi P Y, Peng L F et al. *International Journal of Hydrogen Energy*[J], 2019, 44(5): 3144
- 8 Yi P Y, Zhang W X, Bi F F et al. *Journal of Power Sources*[J], 2019, 410-411: 188
- 9 Yi P Y, Zhang D, Qiu D K et al. *International Journal of Hydrogen Energy*[J], 2019, 44(13): 6813
- 10 Wu M G, Lu C D, Hong T et al. *Surface and Coatings Technology*[J], 2016, 307: 374
- 11 Shi Huiying, Ma Jun, Kang Ying et al. *Rare Metal Materials and Engineering*[J], 2014, 43(3): 621 (in Chinese)
- 12 Larijani M M, Yari M, Afshar A et al. *Journal of Alloys and Compounds*[J], 2011, 509(27): 7400
- 13 Bi F F, Hou K, Yi P Y et al. *Applied Surface Science*[J], 2017, 422(15): 921
- 14 Dong D, Jiang B L, Li H T et al. *Applied Surface Science*[J], 2018, 439: 900
- 15 Ferrari A C, Robertson J. *Physical Review B*[J], 2000, 61(20): 14 095
- 16 Khatir S, Hirose A, Xiao C. *Surface and Coatings Technology* [J], 2014, 253: 96
- 17 Gou W, Li G Q, Chu X P et al. *Surface and Coatings Technology* [J], 2007, 201(9-11): 5043
- 18 Ma T B, Hu Y Z, Wang H. *Carbon*[J], 2009, 47(8): 1953
- 19 Rybachuk M, Bell J M. *Carbon*[J], 2009, 47(10): 2481

质子交换膜燃料电池用 6061 铝合金极板表面类石墨碳涂层的导电耐蚀性能

邵文婷¹, 伍翔宇¹, 蒋百铃², 陈 建¹, 杨 巍¹

(1. 西安工业大学, 陕西 西安 710021)

(2. 西安理工大学, 陕西 西安 710048)

摘 要: 为了获得 6061 铝合金极板表面类石墨碳涂层抗质子酸腐蚀的临界厚度和界面接触电阻的降低量值, 采用磁控溅射方法在 6061 铝合金极板表面制备了一系列类石墨碳涂层。表征了类石墨碳涂层的微观结构, 分析了涂层的界面接触电阻、耐蚀性和稳定性。结果表明, 6061 铝合金极板表面耐质子交换膜燃料电池阴极环境腐蚀的类石墨涂层临界厚度为 $0.97 \mu\text{m}$ 。与低碳靶电流条件下制备的涂层相比, 碳靶电流 4.5 A 时制备的涂层表面更加光滑; 此时, 类石墨碳涂层的界面接触电阻最小, 为 $16 \text{ m}\Omega \cdot \text{cm}^2$, 是石墨极板接触电阻的 2 倍。

关键词: 类石墨碳涂层; 铝合金极板; 界面接触电阻; 耐蚀性

作者简介: 邵文婷, 女, 1988 年生, 博士, 讲师, 西安工业大学材料与化工学院, 陕西 西安 710021, 电话: 029-86173324, E-mail: wenting@xatu.edu.cn